Geochemistry of mafic phenocrysts from alkaline lamprophyres of the Spanish Central System: implications on crystal fractionation, magma mixing and xenoliths entrapment within deep magma chambers

DAVID OREJANA[1,*], CARLOS VILLASECA[1] and BRUCE A. PATERSON[2]

[1] Department of Petrology and Geochemistry, Faculty of Geology, Complutense University of Madrid, 28040 Madrid, Spain
*Corresponding author, e-mail: dorejana@geo.ucm.es
[2] Department of Earth Sciences, University of Bristol, BS8 1RJ, Bristol, UK

Abstract: The Permian alkaline lamprophyres from the Spanish Central System (SCS) are highly porphyritic rocks which carry a heterogeneous population of clinopyroxene and kaersutite zoned phernocrysts. Clinopyroxene phenocrysts may show 1) normal zoning (Cpx-I), 2) reverse zoning with Fe-rich green cores (Cpx-II), and 3) reverse zoning with colourless Al-poor, silica-rich cores (Cpx-III). Kaersutite phenocrysts also show a slight reverse zoning. Major and trace element composition of Cpx-I suggests that their compositional variation is related to a crystal fractionation process from melts similar to the host lamprophyres. The Cpx-II cores represent crystallization from highly evolved melts (low Mg-Cr contents and incompatible element enrichment), genetically related with the SCS alkaline magmatism, and the growth or surrounding Mg-rich inner rims points to a magma mixing process. The major and trace element composition of Cpx-III cores supports derivation from a magma which has fractionated plagioclase. This characteristic, together with their similarities when compared to clinopyroxenes from charnockite xenoliths, suggests that they might be xenocrysts from deep calc-alkaline cumulates. The composition of melts in equilibrium with clinopyroxene and amphibole phenocrysts supports a model in which Cpx-II and Cpx-III cores would have been incorporated into a more primitive lamprophyric magma stagnated at lower crustal levels. The low pressure composition of all phenocryst outer rims indicates that they crystallised directly from the host alkaline magma at their subvolcanic emplacement levels.

Key-words: magma mixing, crystal fractionation, clinopyroxene, amphibole, phenocrysts, alkaline lamprophyres, geochemistry, REE, trace elements, igneous petrology.

Introduction

The heterogeneous major and trace element chemistry shown by mafic phenocrysts from porphyritic basic rocks is a useful tool in determining the processes operating within magma chambers during crystallization, as well as recording the chemical evolution of these melts. Clinopyroxene chemistry is commonly used to infer information on the magma composition from which it crystallised, and several studies for alkaline rocks have focused on this topic using distinct approaches (*e.g.* Dal Negro *et al.*, 1985; Cellai *et al.*, 1994; Tappe, 2004), including in-situ isotope microanalyses (*e.g.* Francalanci *et al.*, 2005).

The presence of chemical zoning in phenocrysts may also help to discriminate between different genetic hypotheses. Such zonation can be caused by changes in mineral-melt equilibria during phenocryst crystallization, as a result of crystal chemistry, or due to crystal growth kinetics (Shimizu, 1990).

Moreover, the complexity of observed phenocryst zoning patterns, normal or reverse, and the formation of multiple rims (*e.g.* Neumann *et al.*, 1999; Xu *et al.*, 2003), usually results from a complex evolutionary process at depth involving multiple magma batches and differentiation in several stages under diverse physico-chemical conditions (Markl & White, 1999). These characteristics have also been explained by mixing after crystallization within more than one magma chamber or by crystallization in a single stratified magma chamber (Wagner *et al.*, 2003).

Clinopyroxene phenocrysts with Fe-rich cores and reverse zoning, showing clear textural and chemical disequilibrium with respect to the host melt, have been explained by a number of different hypotheses (Kollárová & Iván, 2003 and references therein): i) changes in equilibrium crystallisation conditions; ii) changes in melt oxygen and/or water activity; iii) incorporation of accidental xenocrysts; and iv) magma mixing. One of the most frequent fingerprints associated with mixing processes involving basic to ultrabasic magmas is the formation of complex

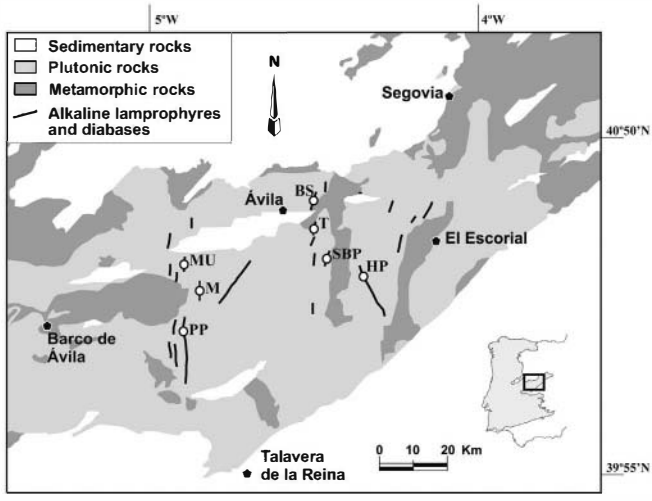

Fig. 1. Geological sketch of the Spanish Central System showing the alkaline lamprophyres crosscutting the granitic-metamorphic basement. The samples with zoned phenocrysts used for the present study have been collected in the outcrops represented with the white circles. BS: Bernuy Salinero; HP: Hoyo de Pinares; M: Maragato: MU: Muñotello; PP: Puerto del Pico; SBP: San Bartolomé de Pinares; T: Tornadizos.

zoning in mafic minerals (mainly clinopyroxene) (Bédard *et al.*, 1988; Dobosi & Fodor, 1992; Xu *et al.*, 2003), though in volatile-rich magmas it also may occur in amphibole (Neumann *et al.*, 1999).

In this study, we describe the chemical variations in major and trace element composition of clinopyroxene and amphibole phenocrysts from the Spanish Central System Permian alkaline lamprophyric dykes. We distinguish different crystal types on the basis of their complex mineral zoning, which can be normal or reverse, the latter usually showing Fe-rich cores giving rise to complexly-zoned clinopyroxene crystals. Crystallization of these phenocrysts is likely to be related to different processes taking place within deep magma chambers, and their heterogeneity points to involvement of highly evolved melts.

Geological background

The Spanish Central System is a Hercynian basement terrain consisting of a large granitic batholith intruded into Neoproterozoic to Palaeozoic metamorphic rocks (Fig. 1). This area has been subsequently cross cut, from the end of the Hercynian collision through to Jurassic times, by different suites of basic dykes of variable affinity (calc-alkaline, shoshonitic, alkaline and tholeiitic; Villaseca *et al.*, 2004). The alkaline dykes constitute a heterogeneous group, which can be divided into: 1) basic to ultrabasic lamprophyres and diabases (which is the one studied in this work) and 2) monzo-syenitic porphyries. Geochronological studies on the SCS alkaline magmatism yield ages in the range from 264 Ma (Ar-Ar in kaersutite; Perini *et al.*, 2004; Scarrow *et al.*, 2006) to 252 Ma (U-Pb in zircon; Fernández Suárez *et al.*, 2006).

The SCS alkaline lamprophyres carry numerous megacrysts (mainly clinopyroxene, amphibole and plagioclase), highlighting the stagnation of these mafic magmas at depth and the involvement of crystal fractionation. They also transport a heterogeneous suite of mafic and ultramafic xenoliths, ranging from pyroxenitic to hornblenditic varieties, interpreted as magmatic cumulates equilibrated at the lower crust-upper mantle boundary and, in some cases, genetically related to the alkaline magmatism (Orejana *et al.*, 2006). Moreover, these dykes are highly porphyritic and show an abundant population of mafic phenocrysts (clinopyroxene, amphibole, phlogopite, olivine pseudomorphs, ülvospinel, *etc.*). Only clinopyroxene and amphibole show compositional zoning. In the San Bartolomé de Pinares outcrops (Fig. 1) clinopyroxene zoning is more complicated; there are allotriomorphic Fe-rich cores and multiple rims, suggesting a complex evolutionary history. Amphibole phenocrysts, which are mainly present in the Tornadizos and Hoyo de Pinares outcrops, but absent in those from San Bartolomé de Pinares, also show Fe-rich cores.

Analytical methods

Concentrations of 29 trace elements (REE, Ba, Rb, Pb, Th, U, Nb, Ta, Sr, Zr, Hf, Y, Cr, Ni, V and Sc) in clinopyroxene and amphibole phenocrysts were determined *in situ* on > 130 μm thick polished sections by laser ablation ICP-MS (LA-ICP-MS) at the *Department of Earth Sciences* (University of Bristol) using a VG Elemental PlasmaQuad 3 ICP-MS coupled to a VG LaserProbe II (266 nm frequency-quadrupled Nd-YAG laser). The diameter of the laser spots was approximately 20–30 μm. The counting time for each analysis was typically 100 s (40 s measuring gas blank to establish the background and 60 s for the remainder of the analysis). The NIST 610 and 612 glass standards were used to calibrate relative element sensitivities for the analyses of the silicate minerals. Each laser analysis used Ca as an internal standard, with concentrations determined by electron microprobe.

Major element mineral compositions were determined at the *Centro de Microscopía Electrónica "Luis Bru" (Complutense University of Madrid)* using a JEOL JZA-8900 M electron microprobe with four wavelength dispersive spectrometers. Analyses were performed with an accelerating voltage of 15 kV and an electron beam current of 20 nA, with a beam diameter of 5 μm. Elements were counted for 10 s on the peak and 5 s on each of two background positions. Corrections were made using the ZAF method.

Petrography

The Spanish Central System alkaline lamprophyres are highly porphyritic, sometimes showing more than 40 % of mafic phenocrysts. The most abundant mafic phenocrysts are clinopyroxene, kaersutitic amphibole and Ti-phlogopite, but other minerals, such as Ti-magnetite-ülvospinel, olivine (normally transformed to secondary talc

group minerals), apatite and ilmenite, may also be present. Plagioclase phenocrysts are only present in the accompanying diabases. The matrix of the alkaline dykes is mainly formed by the same mafic phases present as phenocrysts, plagioclase and, in lower proportions, alkaline feldspar, analcite, calcite, apatite, barite and Fe-sulphides (pyrrotite). Ilmenite is abundant in the matrix or as microphenocrysts in the San Bartolomé de Pinares outcrops, whereas it is scarce in the other dykes studied.

Clinopyroxene and amphibole phenocrysts are the only mafic minerals in these dykes showing clear chemical and petrographic zoning. Figure 2 shows different optic and Back Scattered Electron (BSE) images where zoning characteristics can be observed. Both minerals are idiomorphic to subidiomorphic: amphibole is brown-coloured, displaying hipidiomorphic to allotriomorphic cores (with moderate corrosion textures) and thin darker rims, whereas clinopyroxene is colourless to pale purple (although some have green cores) and has thin purple outer rims. Clinopyroxene tends to show a more variable zoning, with single or multiple rims, sometimes with oscillatory zoning, and idiomorphic to allotriomorphic cores.

On the basis of petrography and major element mineral chemistry we have distinguished two different types of zoning within the clinopyroxene phenocrysts: those with normal zoning (Cpx-I) and those with reverse zoning which present either green cores (Cpx-II) or colourless cores (Cpx-III). Clinopyroxenes with normal zoning have a widespread distribution within the different SCS alkaline dyke swarms, whereas clinopyroxene phenocrysts with reverse zoning are restricted to the San Bartolomé de Pinares outcrops (see location in Fig. 1). Where reverse zoning is observed, it dominates. Reversely zoned amphibole phenocrysts are restricted to the Tornadizos and Hoyo de Pinares dykes (see location in Fig. 1), being absent in the San Bartolomé de Pinares dykes.

In the San Bartolomé de Pinares dyke swarm it is common to find granoblastic charnockitic xenoliths formed by colourless clinopyroxene, plagioclase (normally transformed to sericite), apatite and ilmenite. These enclaves are rounded in shape, equigranular and small in size (usually < 1 cm). They have been recently interpreted as calc-alkaline metabasic cumulates granulitized at lower crustal levels (Villaseca *et al.*, 2007).

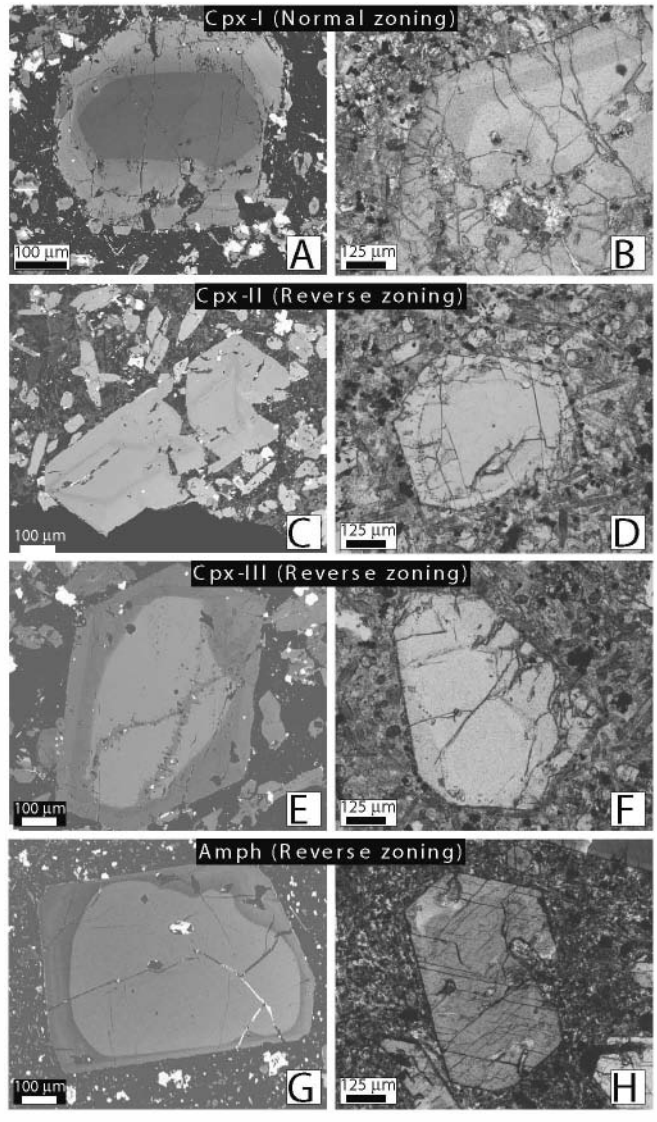

Fig. 2. Back scattered electron and plane polarized light images of clinopyroxene and amphibole phenocrysts. A-B: Clinopyroxene with normal oscillatory zoning (Cpx-I); sample 104403 from Hoyo de Pinares dyke. C-D: Clinopyroxene with reverse zoning and green core (Cpx-II); sample 103657 from San Bartolomé de Pinares dyke. E-F: Clinopyroxene with reverse zoning and colourless core (Cpx-III); sample 103657 from San Bartolomé de Pinares dyke. G-H: Amphibole with reverse zoning; sample 103473 from Tornadizos dyke. Complex zoning with presence of multiple rims is common in these mafic phenocrysts, which usually show allotriomorphic cores.

Phenocrysts chemistry

Major elements

Clinopyroxene is the most abundant phenocryst in the Spanish Central System lamprophyres. Its composition is summarised in Table 1 and 2. They can be classified as Ti-diopsides to Ti-augites. Clinopyroxene with normal zoning (Cpx-I) greatly predominates over those with reverse zoning (Cpx-II and Cpx-III), and is found in all dyke swarms. They are characterised by a heterogeneous composition (considering both cores and rims) with high contents of TiO_2 (0.6–3.3 wt% in cores and up to 5.3 wt% in rims), Al_2O_3 (3.4–11.4 wt%) and CaO (20–25 wt%) (Fig. 3). The variation trend in core composition of these phenocrysts with normal zoning, reflects the differentiation of magma during crystallization. Core Mg# values range from 0.67 to 0.88, and a decrease of SiO_2, CaO and Cr_2O_3 concentration, together with an increase of TiO_2 and Al_2O_3, with decreasing Mg# can be recognised (Fig. 3). Na_2O contents vary mostly between 0.5 and 1.1 wt%, showing a slight inverse correlation with Mg#.

Cpx-I rim compositions follow the same variation trend observed for cores (Fig. 3 and 4). Thus, core to rim zoning

Table 1. Major element composition (expressed as wt%) of clinopyroxene phenocrysts with normal zoning (Cpx-I) from the Spanish Central System alkaline dykes.

Outcrop	Hoyo de Pinares		Maragato				Bernuy Salinero			Puerto del Pico	
Sample	104403		103811				103489			103684	
Analysis #	72	86	37	38	39	40	54	55	56	95	96
	core	rim	core	inner rim 1	inner rim 2	outer rim	core	inner rim	outer rim	core	rim
SiO_2	47.2	42.8	49.9	43.5	45.0	42.6	49.8	44.4	43.0	46.8	43.5
TiO_2	1.98	4.05	1.21	3.88	3.16	4.82	0.66	2.59	3.92	2.10	3.90
Al_2O_3	6.75	9.90	4.52	8.11	6.55	8.97	5.70	10.1	9.50	7.28	7.98
FeO_T*	6.09	7.15	4.17	6.23	5.97	6.95	4.32	7.03	7.69	5.83	6.91
Cr_2O_3	0.27	bdl	0.21	0.16	0.44	bdl	0.84	bdl	bdl	0.06	bdl
MnO	0.14	0.09	bdl	0.08	0.03	0.12	bdl	bdl	bdl	0.06	0.08
NiO	bdl	bdl	0.07	bdl	bdl	bdl	bdl	bdl	bdl	bdl	bdl
MgO	14.2	11.5	16.3	12.9	13.6	11.8	16.7	11.5	10.5	13.8	12.2
CaO	21.6	22.7	23.3	23.9	24.1	23.9	20.4	22.0	23.4	21.9	23.5
Na_2O	0.62	0.48	0.47	0.44	0.33	0.46	0.56	0.86	0.45	0.77	0.49
K_2O	bdl	bdl	bdl	bdl	bdl	bdl	bdl	bdl	0.03	bdl	bdl
Total	98.9	98.7	100.1	99.2	99.2	99.7	99.0	98.5	98.5	98.6	98.6
Mg#	0.81	0.74	0.87	0.79	0.80	0.75	0.87	0.74	0.71	0.81	0.76
P** (GPa)	0.3	0.2	0.1	< 0.1	< 0.1	< 0.1	0.6	0.7	0.0	0.4	< 0.1

* Total Fe expressed as FeO. **Pressure estimates have been calculated using the single-cpx geobarometer of Nimis & Ulmer (1998). bdl: below detection limit.

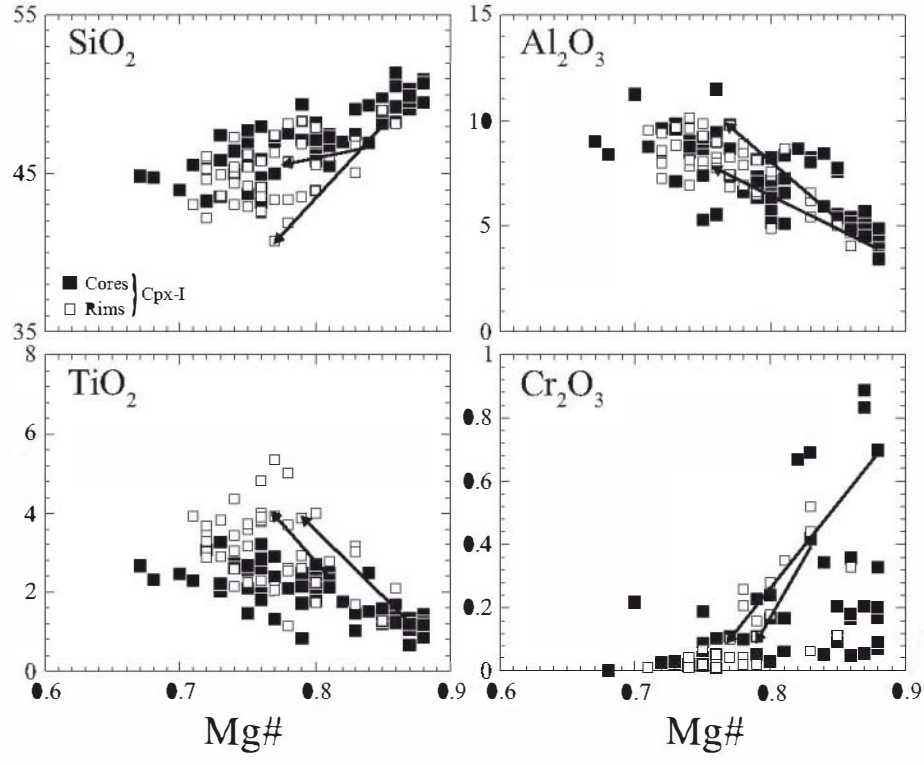

Fig. 3. Major element chemistry of clinopyroxene phenocrysts from the Spanish Central System with normal zoning (Cpx-I). The arrows represent the core to rim zoning trend within single crystals.

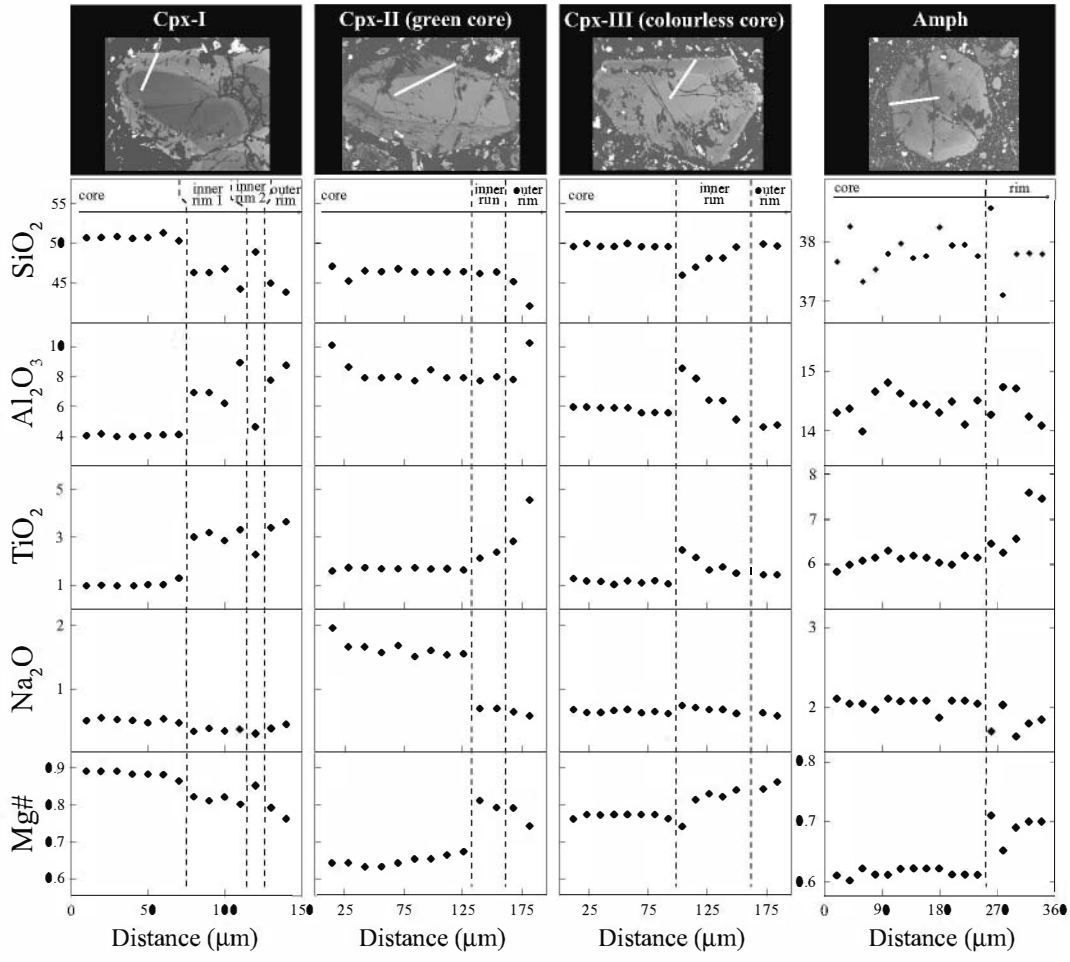

Fig. 4. Core to rim major element variation in clinopyroxene and amphibole phenocrysts from the Spanish Central System. Each column represents the composition of a single crystal analysed by EMP. The crystal is shown at the top as a Back-Scattered Electron image and the white line shows the path followed while analysing. The clinopyroxene with normal zoning is taken from sample 103811 (Maragato), the two clinopyroxenes with reverse zoning from sample 108143B (San Bartolomé de Pinares outcrop) and the amphibole crystal is taken from sample 104403 (Hoyo de Pinares). The vertical dotted lines separate the allotriomorphic core and the surrounding inner and outer rims according to the observed compositional changes.

is characterised by enrichment in Al and Ti and depletion of Si and Cr concentration with decreasing Mg#. Chemical zoning is clearly shown in Fig. 4 where four different sections of Cpx-I, Cpx-II, Cpx-III and amphibole are represented, corresponding with core to rim electron microprobe analyses. Normal zoning in these phenocrysts is occasionally complex, developing several rims around each core which may imply occasional increases in Mg# without significant variation in the other elements (dotted lines in Fig. 4). Sharp chemical changes do exist between zones.

In the San Bartolomé de Pinares outcrop appear reversely zoned clinopyroxene phenocrysts with green cores (Cpx-II) and colourless cores (Cpx-III). Green cores are heterogeneous in Mg-Fe contents, but show high contents of TiO_2 (1.6–2.5 wt%), Al_2O_3 (6.7–9 wt%) and Na_2O (0.7–2.1 wt%) (Table 2; Fig. 5). Green cores display a slight chemical variation trend characterised by depletion of Si, Ca and Cr and enrichment in Al, Na and Ti towards Fe-rich compositions (Fig. 5). They differ from the compositional field drawn by Cpx-I phenocryst (cores and rims) due to their lower Mg# (0.55–0.74) and higher Na concentration (Fig. 5). Cpx-II phenocrysts usually display complex zoning, normally with two rims. The inner rim have higher Mg# (it can reach 0.79–0.83), accompanied by an increase in Ca, Ti and Cr (Cr_2O_3 reaches a maximum of 0.5 wt%) and a decrease in Na (Fig. 4). Formation of the outer rim involves decreases in Si, Na and Mg# (0.76–0.8), and increases in Ti and Ca with respect to the inner rim. The major element composition of these rims clearly overlaps the composition of matrix clinopyroxenes from the same samples (Fig. 5).

Colourless clinopyroxene cores also show a heterogeneous composition in terms of Mg# (0.57–0.88), Al_2O_3 (1.4–7.5 wt%), TiO_2 (0.1–1.5 wt%) and Na_2O (0.1–1.36 wt%), and high silica contents (SiO_2 = 48–52 wt%) (Fig. 5). They differ significantly from the other clinopyroxene phenocryst cores due to lower Ti, Na and Al, and higher Si concentrations. The major element composition of colourless cores give rise to a variation trend characterised by depletions of Al, Ti, Ca, Na and Cr, with

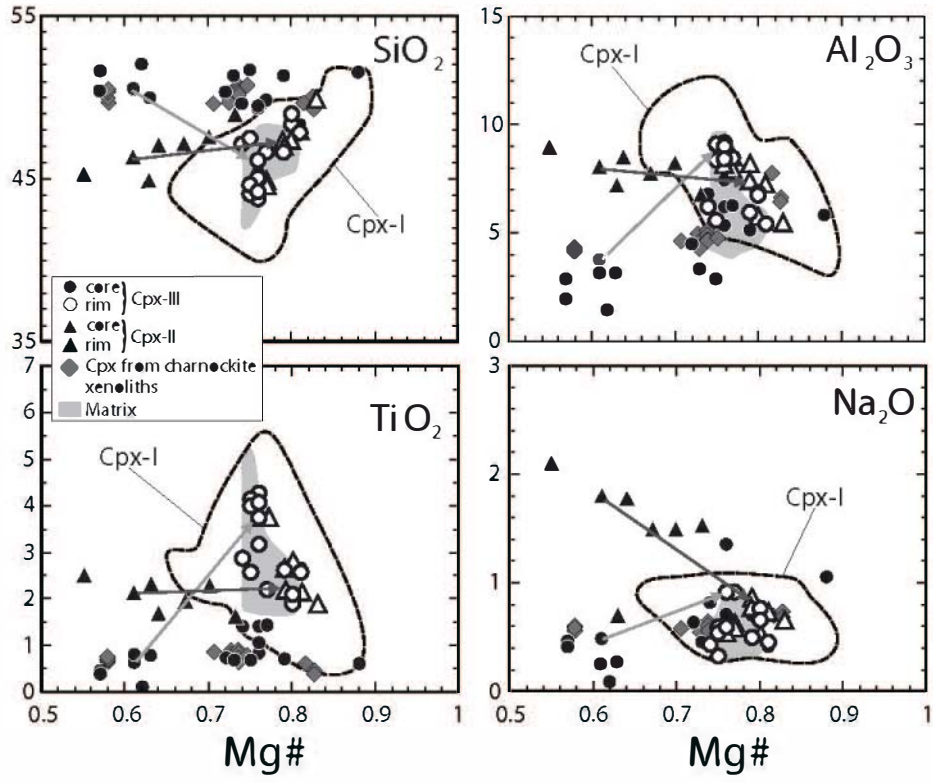

Fig. 5. Major element chemistry of reversely zoned clinopyroxene phenocrysts (Cpx-II and Cpx-III) from the Spanish Central System compared with composition of Cpx-I (cores and rims) and matrix clinopyroxenes in the same samples. Major element contents of groundmass clinopyroxenes represent authors' unpublished data. Arrows represent the core to rim zoning within a single crystal. For comparison it has also been plotted the compositional range of clinopyroxenes from charnockite xenoliths present in San Bartolomé de Pinares outcrop.

decreasing Mg# (Fig. 5). As observed for the Cpx-II phenocrysts, these usually show similarly complex zonation. From core to the inner rim we observe increases in Mg#, Ti, Al and Na contents, and depletion in Si (Fig. 4), which imply the presence of a sharp contact. The fact that this change appears at slightly shorter distances from the crystal border in the case of Mg# could probably be explained by a diffusion process. Their rim composition displays a continuous change with increasing Si and Mg, and decreasing Al, Ti and Na (Fig. 4). Cpx-III phenocryst rims also show a similar composition to that of matrix clinopyroxenes from the same alkaline dykes (Fig. 5).

It is interesting to note that the major element composition of clinopyroxenes from the charnockite xenoliths present in the San Bartolomé de Pinares outcrop is very similar to the most Fe-rich colourless cores (Fig. 5), suggesting a genetic relationship between them.

Amphibole phenocrysts are Ti-rich kaersutites. They give rise to a relatively homogeneous compositional range with Mg# from 0.60 to 0.72 and high TiO_2 (5.1–7.7 wt%) and Al_2O_3 (13.1–14.8 wt%) contents (Table 3). Na_2O and K_2O concentrations range from 1.7 to 2.6 wt% and from 1.1 to 2.4 wt% respectively. All amphibole analyses describe a broad compositional trend mainly characterised by increasing Ti, Ca and Cr and decreasing Al concentrations towards higher Mg#, which also represent the core to rim chemical zoning (Table 3; Fig. 6). Zoning in amphibole phenocrysts is always reverse (Fig. 4). The rim shows enrichment in Ti and slightly lower Na contents, in accordance with the general compositional trend, as represented in Fig. 6. Clinopyroxene phenocrysts from Hoyo de Pinares dyke coexisting with amphibole phenocrysts, on the contrary, show progressive normal zoning. In both minerals the core to rim chemical variation displays the same trend: Cr and Na decrease and Ca, Ti and Al^{IV}/Al^{VI} increase (Table 1 and 3). Amphibole rims clearly show a similar major element composition to that of matrix kaersutites from the same alkaline dykes (Fig. 6).

Trace elements

The trace element composition of Cpx-I phenocrysts is characterised by high HFSE (except Nb) and REE concentrations (Table 4), displaying chondrite-normalised patterns with convex upward shapes and primitive mantle-normalised patterns with negative Ba, Nb, Pb and Sr anomalies (Fig. 7). Rims are enriched in most trace elements when compared to core concentrations (Sr, Ta, Nb, Zr, Y, V and REE) (Table 4).

Cpx-II phenocryst core trace element contents overlap those of Cpx-I, but generally have higher concentrations (Fig. 7A). Their inner rims are generally depleted in trace elements with respect to core composition, but the outer

Table 2. Major element composition (expressed as wt%) of clinopyroxene phenocrysts with reverse zoning and accompanying charnockite xenoliths from the Spanish Central System alkaline dykes.

Outcrop	San Bartolomé de Pinares											
Type	Green cores (Cpx-II)					Colourless cores (Cpx-III)					Xenoliths	
Sample	104534A		L104534A			103658			L104534A		L104534	108143B
Analysis#	41	42	79	80	81	63	64	65	66	67	86	72
	core	rim	core	inner rim	outer rim	core	inner rim	outer rim	core	rim		
SiO_2	47.1	47.7	48.8	49.9	45.6	50.3	46.6	43.8	50.5	46.1	50.0	50.1
TiO_2	1.72	2.40	1.62	1.84	3.73	0.74	2.18	4.26	0.63	3.16	0.66	0.37
Al_2O_3	8.45	6.72	6.78	5.45	8.16	4.51	8.51	9.21	3.83	9.05	4.13	6.46
FeO_T*	9.61	6.22	7.50	5.35	6.86	9.13	6.78	6.74	12.9	6.92	14.1	5.39
Cr_2O_3	0.09	0.26	0.04	0.49	bdl	bdl	0.21	bdl	bdl	0.04	bdl	bdl
MnO	0.10	0.12	0.14	0.12	0.23	0.03	0.05	0.03	0.21	0.09	0.21	0.18
NiO	bdl	bdl	bdl	bdl	0.05	bdl	0.05	bdl	bdl	0.10	bdl	bdl
MgO	9.62	13.5	11.1	14.4	12.1	13.3	13.0	11.8	11.3	12.0	11.0	14.7
CaO	21.3	22.3	22.7	23.2	24.0	20.3	21.2	23.3	20.3	22.4	19.7	22.1
Na_2O	1.79	0.63	1.53	0.64	0.52	0.64	0.91	0.63	0.49	0.91	0.57	0.70
K_2O	bdl	bdl	bdl	bdl	bdl	bdl	bdl	bdl	bdl	bdl	bdl	bdl
Total	99.8	99.9	100.3	101.4	101.3	99.0	99.5	99.8	100.1	100.8	100.4	100.0
Mg#	0.64	0.79	0.73	0.83	0.76	0.72	0.77	0.76	0.61	0.76	0.58	0.83
P** (GPa)	0.7	0.2	0.5	0.2	< 0.1							

* Total Fe expressed as FeO. **Pressure estimates have been calculated using the single-cpx geobarometer of Nimis Ulmer (1998). Cpx-III and clinopyroxenes from charnockitic xenoliths have not been considered for P calculations because they have not crystallized from basic-ultrabasic magmas. bdl: below detection limit.

Table 3. Major element composition (expressed as wt%) of amphibole phenocrysts from the Spanish Central System alkaline lamprophyres.

Outcrop	Tornadizos					Bernuy Salinero	Muñotello	Hoyo de Pinares		
Sample	80318	103473			103474	103488	L103818	104403		
Analysis#	4	1	15	17	78	1	5	62	68	71
	core	core	inner rim	outer rim	core	core	core	core	inner rim	outer rim
SiO_2	37.8	37.9	38.7	39.0	38.5	38.2	38.7	37.8	37.1	37.8
TiO_2	6.09	5.91	5.72	6.06	5.64	6.23	5.08	6.15	6.25	7.44
Al_2O_3	14.5	14.5	13.6	13.2	14.3	14.9	13.4	14.4	14.7	14.1
FeO_T*	12.3	11.0	10.5	9.69	11.6	10.5	12.4	12.0	11.4	9.64
Cr_2O_3	0.04	bdl	0.03	bdl	bdl	bdl	bdl	bdl	bdl	bdl
MnO	0.12	0.15	0.15	0.07	0.07	bdl	0.18	0.17	0.12	0.10
MgO	11.2	11.5	12.4	13.0	10.7	10.8	11.6	11.0	11.8	12.4
CaO	11.4	11.1	12.1	12.4	11.9	11.7	11.9	11.8	11.8	12.6
Na_2O	1.88	1.72	1.75	1.83	1.88	2.56	1.99	2.08	2.02	1.84
K_2O	2.14	2.19	2.11	1.95	2.02	1.50	2.16	1.94	1.96	1.67
Total	97.5	96.1	97.1	97.1	96.6	96.4	97.4	97.3	97.1	97.5
Mg#	0.62	0.65	0.68	0.70	0.62	0.65	0.62	0.62	0.65	0.70

* Total Fe expresed as FeO. bdl: below detection limit.

rims are enriched (Table 4). The chemical trend observed from inner to outer rim in these crystals is similar to that shown by Cpx-I, with the exception of V which shows no clear zoning trend (Table 4).

Cpx-III phenocryst cores also display a trace element composition close to that of Cpx-I cores, but they are strongly Y-REE enriched (Fig. 7A,B) and have remarkably large negative Eu anomalies in their chondrite-normalised REE patterns. Moreover, they also have deep negative Nb-Ta, Ti, Pb and Sr anomalies in the primitive mantle-normalised patterns (Fig. 7A,B). The rims are enriched in trace elements with respect to the cores in most cases, except for Y and REE (Table 4). As mentioned above for major elements, the trace element composition of clinopyroxenes from the charnockite xenoliths is very similar to that of the Cpx-III cores, showing the same Y-REE enrichment and deep negative Nb-Ta, Ti, Sr and Eu anomalies (Fig. 7A,B).

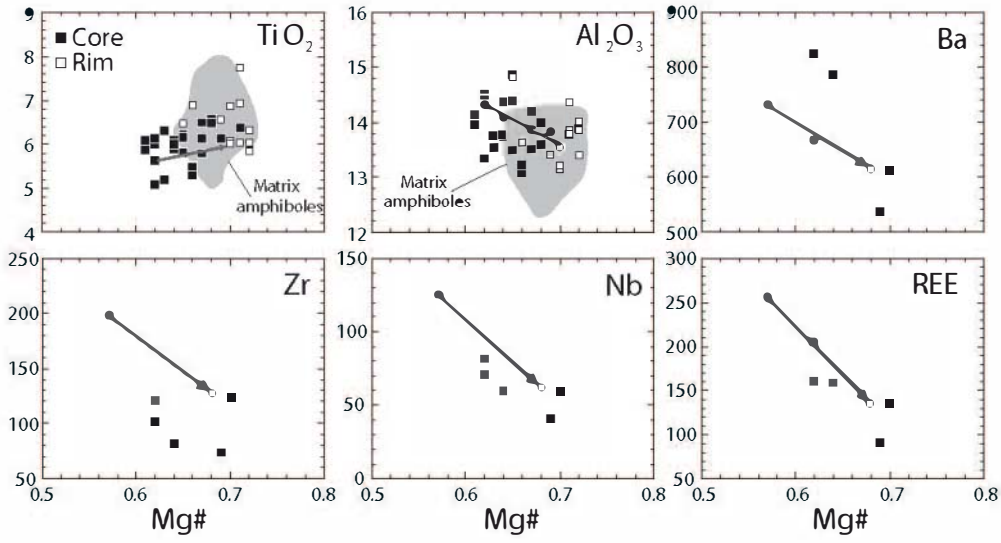

Fig. 6. Major and trace element chemistry of amphibole phenocrysts from the Spanish Central System. The arrow represents the general core to rim zoning trend within crystals. Compositional range of matrix ampbiboles from SCS host dykes are taken from authors' unpublished data.

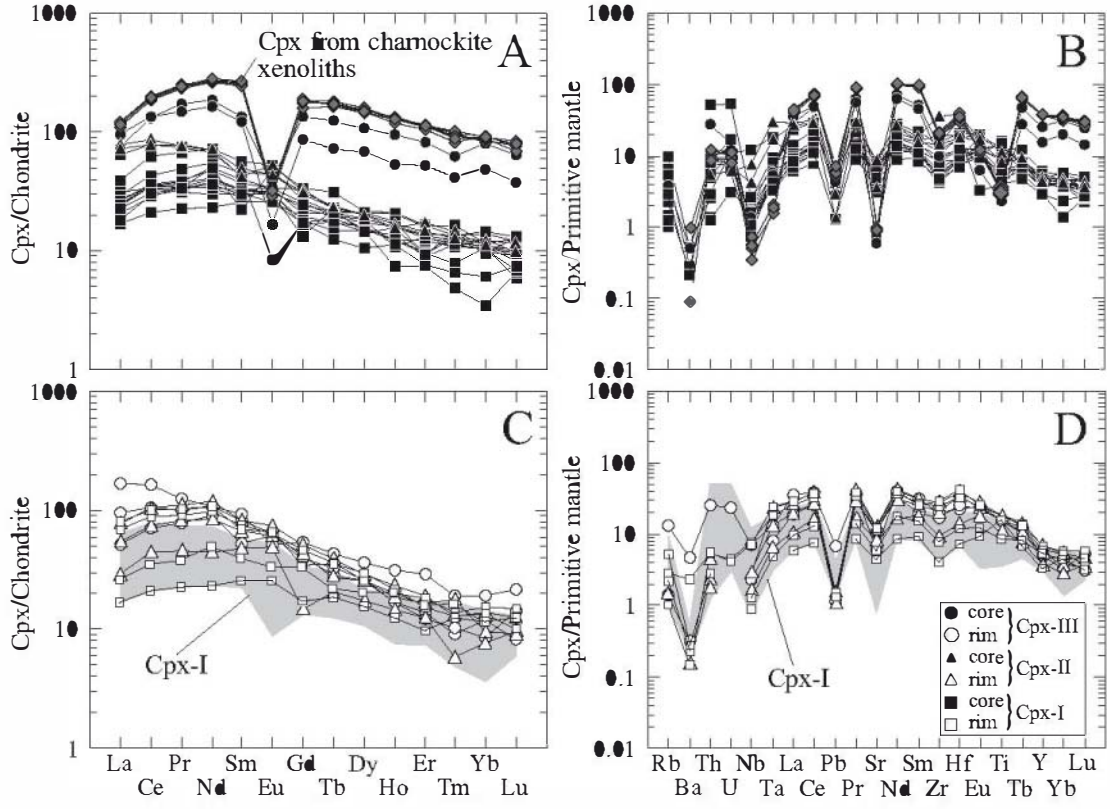

Fig. 7. A, B: Chondrite and primitive mantle normalised trace element composition of cores from clinopyroxene phenocryst with normal and reverse zoning, and clinopyroxenes from charnockite xenoliths. C, D: Chondrite and primitive mantle normalised trace element composition of rims from clinopyroxene phenocryst with normal and reverse zoning, compared to compositional range of Cpx-I cores. Chondrite and primitive mantle normalising values after Sun & McDonough (1989) and McDonough & Sun (1995), respectively.

Table 4. Trace element concentrations (ppm) of clinopyroxene phenocrysts and clinopyroxenes from accompaning charnockite xenoliths from the Spanish Central System alkaline dykes.

Outcrop	Bernuy Salinero	Tornadizos			Muñotello		San Bartolomé de Pinares											
Type		Normal zoning (Cpx-I)						Green cores (Cpx-II)					Colourless cores (Cpx-III)				Xenoliths	
Sample	103471	103473			103818		L104534	L104534A					L104534A				L104534	
Analysis #	18	1	8	13	2	9	2	4	5	6	11	12	7	8	1	3	5	9
	core	core	core	core	core	rim	rim	core	inner rim	outer rim	core	rim	core	rim	core	rim		
Rb	1.33	0.61	0.76	bdl	3.83	3.22	1.71	bdl	0.93	bdl	bdl	bdl	bdl	7.99	2.26	0.87	bdl	bdl
Ba	1.50	bdl	bdl	bdl	bdl	1.91	15.55	bdl	bdl	1.07	bdl	bdl	bdl	30.78	3.33	2.12	6.33	bdl
Th	bdl	0.10	0.11	bdl	0.20	0.23	0.42	0.88	0.14	0.19	0.43	0.36	2.20	2.04	0.62	bdl	0.700	0.814
U	bdl	bdl	bdl	bdl	bdl	bdl	0.09	bdl	bdl	bdl	0.12	bdl	0.30	0.48	0.15	bdl	0.164	0.234
Ta	bdl	0.36	0.29	0.13	0.12	0.18	0.67	0.63	0.25	0.49	1.09	0.86	0.20	0.49	0.22	0.30	0.065	0.058
Nb	0.60	1.60	1.18	1.11	1.07	0.85	5.00	2.87	1.10	1.95	4.77	2.93	0.62	4.68	0.89	1.51	bdl	0.335
Sr	89.4	168.1	163.9	134.4	109.2	117.8	220.4	176.1	161.8	226.3	69.8	251.0	12.1	120.5	93.2	215.8	19.14	17.88
Pb	na	na	na	na	na	na	0.23	0.21	bdl	0.24	0.43	0.17	0.64	1.01	0.43	0.17	0.881	0.894
Hf	2.08	5.79	4.90	3.72	2.78	3.44	9.29	4.96	3.81	9.66	10.99	10.97	5.08	5.73	8.77	7.32	10.6	8.983
Zr	43.1	153.0	122.1	89.3	51.0	85.6	251.6	152.6	98.5	221.2	376.0	287.2	104.0	132.7	151.6	179.6	211.9	205.1
Y	14.3	25.9	21.4	12.6	20.0	24.2	29.5	19.7	16.6	23.8	20.7	28.7	65.9	37.4	108.9	21.7	164.1	160.2
V	393	383	366	357	506	503	255	285	267	251	283	291	322	335	567	239	574.1	574.3
Sc	na	na	na	na	na	na	74	54	70	77	49	82	39	55	120	72	145.9	143.9
Ni	227	94	110	38	182	75	na	na	na	na	na	na	na	na	na	na	na	na
Cr	6117	84	84	87	607	99	53	130	1431	85	122	80	316	652	280	274	184.5	184.7
Ti*	19184	14988	16187	17985	7494	10491	na	13578	12769	na	9711	22385	2751	12541	3788	18980	4376	3417
La	3.97	9.23	6.90	4.93	4.35	6.26	16.18	17.20	6.96	12.90	18.63	18.05	22.83	22.44	17.73	12.23	28.92	28.94
Ce	12.78	37.95	26.30	17.46	17.64	21.88	54.59	47.98	27.23	45.07	52.93	63.67	82.39	63.54	79.36	43.01	122.30	118.80
Pr	2.18	6.37	4.66	3.28	3.15	3.63	8.51	7.38	4.25	7.71	7.30	10.55	14.00	9.48	16.20	7.39	23.42	22.88
Nd	10.91	34.24	25.93	18.84	18.02	23.08	45.59	33.41	20.60	39.28	33.08	55.07	77.41	49.70	87.63	42.09	126.30	123.10
Sm	3.89	8.60	6.87	5.00	5.02	6.20	11.32	6.41	7.36	10.33	7.47	12.64	18.56	14.06	20.45	8.00	38.46	38.19
Eu	1.48	3.04	2.54	1.78	1.97	1.97	3.76	3.08	2.84	3.53	2.57	4.28	0.98	2.96	2.27	3.50	1.70	1.86
Gd	3.58	6.98	6.11	3.77	5.24	6.95	9.58	6.60	2.99	8.87	6.45	10.66	17.68	11.03	27.90	7.94	37.71	38.03
Tb	0.70	1.18	0.87	0.56	0.74	0.83	1.35	0.88	0.77	1.00	0.90	1.48	2.70	1.61	4.64	1.24	6.33	6.49
Dy	3.96	5.54	5.13	3.75	4.40	5.25	6.45	5.05	4.41	6.49	5.07	7.40	17.58	9.14	27.07	6.76	39.49	37.76
Ho	0.71	1.19	0.89	0.43	0.91	1.17	1.14	0.90	0.82	1.05	0.95	1.33	3.08	1.78	5.38	0.96	7.33	7.23
Er	1.61	2.69	2.22	1.23	2.13	2.66	3.04	2.83	2.07	2.71	2.38	3.13	8.70	4.84	13.72	2.02	19.03	18.38
Tm	0.32	0.34	0.32	0.12	0.30	0.42	0.36	0.37	0.15	0.46	0.33	0.33	1.07	0.49	1.58	0.26	2.47	2.35
Yb	1.96	2.36	1.83	0.60	1.89	2.00	2.57	1.89	1.28	1.61	2.08	2.35	8.61	3.27	13.57	1.44	15.95	14.68
Lu	0.22	0.31	0.21	0.17	0.26	0.32	0.38	0.25	0.24	0.23	0.30	0.32	0.97	0.55	1.63	0.36	1.93	1.92

* Ti concentrations have been obtained form EMP analyses. na: not analysed; bdl: below detection limit

The trace element composition of amphibole phenocryst cores is in a limited range (Table 5) and it is very similar to that of the only rim analysed (Fig. 8). They yield convex upward chondrite-normalised REE patterns, similar to those of the coexisting clinopyroxene phenocrysts. This shape is typical of deep cumulates formed from basaltic melts (Irving & Frey, 1984). They are highly enriched in the most incompatible trace elements, LILE (mainly Ba = 537–826 ppm), HFSE (Nb = 40–126 ppm; Ta = 2.3–5.6 ppm; Zr = 72–199 ppm) Sr (872–1152 ppm) and REE (90–256 ppm) (Table 5), and thus primitive mantle-normalised trace element patterns show strongly positive Ba, Nb-Ta, Ti and Sr anomalies, also accompanied by a negative Th-U anomaly (Fig. 8). Nonetheless, the trace element data of cores and rims also display a clear compositional trend; an increase in Mg# is accompanied by a decrease in the concentration of most trace elements (with the exception of Rb and V) (Fig. 6; Table 5).

Origin of the chemical variation and zoning in phenocrysts

Fractional crystallization

Clinopyroxene composition is controlled by either physical conditions of crystallization (pressure, temperature) and/or parameters related with the geochemical composition of the parent magma, as shown by different crystal-chemical studies (*e.g.* Dal Negro *et al.*, 1985, 1986; Cellai *et al.*, 1994). Some detailed works made on Mediterranean alkaline rocks (mainly potassic and ultrapotassic suites) have stated that chemical variations in clinopyroxene crystals from a wide range of cogenetic magmatic compositions can be used as petrological tracers (Avanzinelli *et al.*, 2004). Nevertheless, the SCS basic to ultrabasic alkaline magmas show a short silica range (41.2–45.7 wt%). This suggests that other factors, besides the chemical composition of the parental magma, should have controlled the chemical differences displayed by this complex association of clinopyroxene phenocrysts.

Two different hypotheses might be advocated to explain the presence of normal zoning in clinopyroxene phenocrysts (Cpx-I) from the SCS alkaline lamprophyres, with trends towards higher Fe, Al, Ti and Na and lower Mg and Cr contents from core to rim: 1) magma differentiation as a consequence of progressive cooling and crystallization, and 2) changes in pressure conditions during crystallization.

Yagi & Onuma (1967), Aoki & Kushiro (1968), Kushiro (1969) and Wass (1979), have indicated that pressure may act as a dominant factor in controlling the composition of clinopyroxenes formed from basic magmas at depth, so that increasing pressure would be followed by increasing Na and Al^{VI} content in cpx, whilst a decrease in pressure would show a negative correlation towards higher Ti and Al^{IV} concentrations. Clinopyroxenes with normal zoning (Cpx-I) in this study show outer rims with lower $Na+Al^{VI}$ concentrations and higher $Ti+Al^{IV}$ when compared to core composition. If we consider the Al^{VI} *vs.* Al^{IV} diagram of Aoki & Kushiro (1968), these rims would plot within the lower pressure field (igneous rocks), in accordance with the hypothesis involving changes in pressure conditions. Nevertheless, this factor does not seem to be significant in the case of most of inner rims, which show $Na + Al^{VI}$ and $Ti + Al^{IV}$ similar to core values, and would plot within the intermediate pressure field (inclusions in basalts) of Aoki & Kushiro (1968). This likely indicates that normal zoning is influenced by other factors besides pressure.

The compositional trend displayed by Cpx-I and amphibole phenocryst cores from the Spanish Central System is in favour of a crystal fractionation process involving depletion of magma in Mg, Cr, Si and Ca, and enrichment of Al and incompatible trace elements (Fig. 3 and 6), and this might be produced by crystallization of ol + cpx ± Cr-sp. The presence of abundant cpx phenocrysts and pseudomorphed olivine, together with minor proportions of small Cr-spinel microphenocrysts, within the SCS alkaline mafic dykes, reinforces this possibility. All major elements, with the exception of Ti, behave in a similar way when considering those phenocryst cores (Cpx-I and amphibole). The increment of the Ti concentration in Cpx-I cores towards more evolved compositions (Fig. 3) means an increasing content of this element in the residual magma. Nevertheless, fractionation of kaersutite + Ti-phlogopite ± ülvospinel (common phenocrysts in amphibole-bearing dykes), could account for the Ti decrease in amphibole cores towards lower Mg#. These minerals would have been the dominant crystallising phases after (or during) the removal of ol + cpx.

The presence, within Cpx-I phenocrysts, of a slight increase in Mg# from inner rim 1 to inner rim 2, accompanied by slight changes in the variation trends for other elements (Ti, Al and Na; Fig. 4), could be explained by the incorporation of these crystallising phases in a more primitive magma batch. This probably indicates that phenocrysts coming from diverse zones of a single magma chamber might have been trapped by a more primitive ascending melt (maybe due to convection) with a similar composition to the one that formed the phenocryst cores.

Thus, core to rim chemical zoning in Cpx-I phenocrysts from SCS alkaline dykes suggests that a crystal fractionation process is the dominant control. This could explain decreases in Mg and Cr and increase in Fe, Ti, Al and Na from core to inner rims. Nevertheless, a drop in pressure during crystallization, possibly related to magma transport and intrusion at higher crustal levels, would be in accordance with the lower Na and Al^{VI} concentrations of the outer rims. A similar fractionating mineral assemblage could account for the variation observed in amphibole cores, though Ti-phases such as Ti-phlogopite and ülvospinel, might have also been involved as indicated by the negative correlation of Fe/Mg ratio and Ti content in kaersutite cores (Fig. 6).

Magma mixing and xenocrysts entrapment

Generation of reverse zoning within clinopyroxene crystals in alkaline rocks is widely documented, including studies focused on clinopyroxenes with Fe-rich green cores (Brooks & Printzlau, 1978; Wass, 1979; Duda &

Table 5. Trace element composition (ppm) of amphibole phenocrysts from the Spanish Central System alkaline lamprophyres.

Outcrop	Tornadizos					Muñotello	
Sample	103473					103818	
Analysis #	4	5	6	7	12	5	6
	core	rim	core	core	core	core	core
Rb	16.24	18.52	18.64	13.54	13.67	16.71	14.46
Ba	732	613	538	666	610	825	786
Th	0.122	bdl	bdl	0.132	0.164	0.206	0.277
U	bdl	bdl	bdl	bdl	bdl	0.101	bdl
Ta	5.60	3.36	2.34	3.28	3.27	3.50	2.62
Nb	125.4	61.8	40.5	70.27	58.89	81.46	59.71
Sr	1152	1017	873	1134	1036	964	1000
Hf	5.91	4.16	2.34	3.36	4.25	4.14	3.58
Zr	198.5	126.8	72.7	120.4	123.5	102	81.4
Y	38.93	19.15	15.54	26.61	22.59	39.97	33.4
V	446.8	604	547.8	462.4	488.9	523.6	560.6
Ni	bdl	68.86	149	78.17	32.28	139.9	136.5
Cr	bdl	14.94	107.4	43.1	16.01	68.44	90.17
Ti*	32612	39866	38907	37468	38547	30454	35970
La	26.20	13.66	8.64	16.18	14.27	19.99	15.15
Ce	86.82	45.71	28.29	54.52	45.00	67.49	49.73
Pr	13.66	6.83	4.75	8.76	7.09	10.40	7.95
Nd	70.57	38.80	25.36	45.62	38.16	58.94	44.27
Sm	16.45	8.67	6.61	10.04	8.06	13.03	11.46
Eu	4.66	3.24	2.29	3.78	3.23	3.98	3.45
Gd	13.41	6.31	5.00	8.06	6.68	11.51	8.47
Tb	1.83	1.11	0.76	1.14	1.01	1.39	1.13
Dy	10.71	5.02	3.91	5.96	5.32	9.11	8.03
Ho	2.03	0.98	0.85	1.17	0.98	1.72	1.30
Er	4.48	1.81	1.63	2.55	2.64	3.53	4.19
Tm	0.57	0.36	0.34	0.32	0.25	0.67	0.45
Yb	4.20	1.46	1.85	2.30	1.97	3.31	2.61
Lu	0.48	0.27	0.21	0.34	0.17	0.39	0.40

* Ti concentrations have been obtained from EMP analyses. na: not analysed; bdl: below detection limit

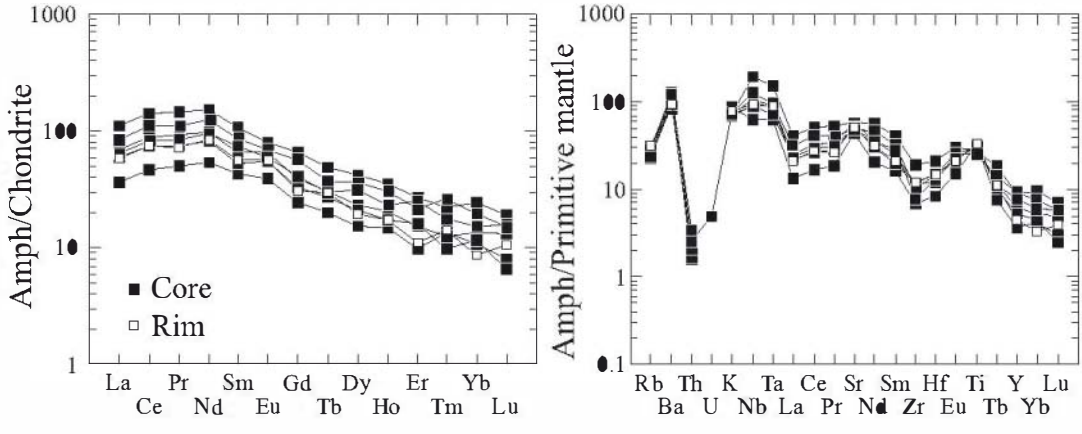

Fig. 8. Chondrite and primitive mantle normalised trace element composition of amphibole phenocryst from the Spanish Central System alkaline dykes. Chondrite and primitive mantle normalising values after Sun & McDonough (1989) and McDonough & Sun (1995), respectively.

Schmincke, 1985; Bédard *et al.*, 1988; Neumann *et al.*, 1999; Xu *et al.*, 2003; Tappe, 2004). The presence within the Spanish Central System alkaline dykes of clinopyroxene phenocrysts with reverse zoning and corroded Fe-rich cores implies that crystal fractionation is not sufficient to explain their complex zoning patterns and that other processes must have been involved. Nevertheless, it is important to note that these clinopyroxenes only occur in the San Bartolomé de Pinares outcrop, whilst reversely zoned amphiboles appear in the Tornadizos and Hoyo de Pinares outcrops.

The chemical changes from core to inner rim in green-core Cpx-II from San Bartolomé de Pinares, together with the Cr, Na and Al variations observed, are consistent with the mixing of magmas with different degrees of evolution. The same has also been interpreted in similar zoning patterns of Fe-rich clinopyroxene cores, leaving aside the question of their cogenetism (Brooks & Printzlau, 1978; Bédard *et al.*, 1988; Dobosi & Fodor, 1992; Neumann *et al.*, 1999; Xu *et al.*, 2003). Mixing may occur between distinct magma batches or between different zones of a same magma chamber, through a convective self-mixing process (*e.g.* Couch *et al.*, 2001). The fact that Cpx-I and Cpx-II display high Ti and incompatible trace elements concentrations, suggests that they must be related to alkaline melts, genetically linked with the host SCS alkaline lamprophyres.

As it has been marked in Fig. 5, green (Cpx-II) and colourless (Cpx-III) cores display different compositional variation trends that tend to converge towards the field of clinopyroxenes with normal zoning (Cpx-I) for the highest Mg# values (Fig. 5). Cpx-II cores are Cr-poor and describe a compositional trend analogous to that of Cpx-I cores (decrease of Si and Ca and increase of Al and Na), though following a different slope, and, in addition, Cpx-II cores tend to more Fe-rich compositions (Fig. 5). This suggests that the two magmas involved in their origin evolved as a consequence of fractionation of a similar mineral assemblage (olivine + clinopyroxene ± Cr-spinel).

Kaersutite reverse zoning also supports the mixing hypothesis, although it is important to note that amphibole phenocrysts are absent in the San Bartolomé de Pinares outcrops, which show reversely zoned Cpx-II and Cpx-III crystals. The major and trace element contents of amphibole rims closely resemble that of phenocrysts cores, without the existence of an abrupt compositional gap (Fig. 6 and 8) or any observed corrosion texture between amphibole cores and rims, thus indicating that only a slight chemical disequilibrium affected these phenocrysts. Moreover, rims seem to follow the same trend described by core analyses (Fig. 6). These characteristics point to amphibole phenocryst cores and rims being formed from melts with similar compositions, though the increase in Mg# would indicate incorporation of crystallising amphiboles in a more primitive ascending alkaline magma. Clinopyroxene phenocrysts coexisting with amphiboles in a single thin section display normal zoning. The Al^{IV}/Al^{VI} ratio and Ti content significantly increase towards rim in clinopyroxene and amphibole phenocrysts, supporting rim crystallization at lower pressures in both cases. The different core to rim behaviour of Mg# in these phenocrysts probably indicates that they are not strictly cogenetic, but that a cpx-rich magma incorporated, during its ascent, amphibole phenocrysts formed at depth from a more evolved melt.

The trend outlined by Cpx-III cores is significantly different, showing a decrease in Al, Ti, Ca, Cr and Na with decreasing Mg# (Fig. 5). The low Al, Ca and Na contents in these Cpx-III cores is probably influenced by fractionation of plagioclase, whilst the decrease in Ti could be related to ülvospinel or ilmenite crystallization. The strong Y-REE enrichment, together with the deep negative Sr and Eu anomalies in their trace elements patterns shown by these clinopyroxenes, all support plagioclase co-crystallization and are in accordance with a derivation from a more evolved melt (Neumann *et al.*, 1999). This contrasted evolutionary pattern supports the involvement of a third magmatic component, but it is highly unlikely that it would be linked with any alkaline melt, due to the Al-Ti-poor composition of Cpx-III. Taking into account that no other magmatic event occurred in the SCS during lamprophyre genesis and intrusion, we favour a xenocrystic origin for Cpx-III cores. Accordingly, reverse zoning in these phenocrysts could not be ascribed to mixing but inclusion of solid material, a possibility which has been previously suggested in similar rocks (Wass, 1979).

The San Bartolomé de Pinares outcrop, where Cpx-III phenocrysts may be found, also include plagioclase-bearing xenoliths of charnockite affinity (Villaseca *et al.*, 2007). There is an evident resemblance between the major and trace element composition of clinopyroxenes from these xenoliths and Cpx-III colourless cores, including the deep Eu and Sr anomalies (Fig. 5 and 7), which is indicative of crystallization from a magma batch that involve plagioclase fractionation. The fractionating mineral assemblage proposed above for Cpx-III cores coincides with the modal composition of the associated enclaves, which supports that Cpx-III cores were incorporated into the alkaline magma as fragments of the charnockite xenoliths.

Rims from every clinopyroxene phenocryst (with normal or reverse zoning) give rise to a relatively homogeneous compositional field, both for major and trace elements (Fig. 5 and 7). This similarity in inner and outer rims of clinopyroxene phenocrysts, indicates that all rims formed from a similar magma, after incorporating clinopyroxene cores from different origins. The presence within a single thin section of a heterogeneous clinopyroxene phenocryst population with complex zoning, has previously been explained by magma mixing after crystallization from different melts (Wagner *et al.*, 2003). The fact that some crystals with normal zoning show multiple rims with successive variations of Mg# (increasing and decreasing towards the outer rim), probably represents episodic involvement of more primitive magma batches within the magma chamber, prior to dyke intrusion. Entrainment of new and more primitive melts into the magma chamber could have given rise to magma mixing and incorporation of xenocrystic material and previously crystallised clinopyroxene phenocrysts, derived from more evolved melts and recording different magma chamber levels. These phenocrysts would have been partially dissolved as a result of mixing with this

new magma batch, resulting in formation of allotriomorphic cores and, eventually, more clinopyroxene would have nucleated on these cores giving rise to Mg-rich inner and outer rims.

Pressure estimates on Cpx-I cores obtained using the single-cpx geobarometer of Nimis & Ulmer (1998) yield ranges mainly from 0.3 to 0.8 GPa, and P values for their outer rims are generally lower than 0.1 GPa (Table 1). The wide range of pressure estimations for Cpx-I cores suggests that the alkaline melts of each dyke swarm might have stagnated within a magma chamber at fairly different depths. For instance Cpx-I cores from Maragato outcrop seem to have crystallised at subvolcanic levels, whereas those from Bernuy Salinero equilibrated near 20 km in depth (Table 1).

Pressure estimates for Cpx-II cores gives values up to 0.7 GPa (Table 2), which might represent minimum crystallization conditions. Cpx-III does not derive from basic-ultrabasic magmas, which is a requirement of Nimis & Ulmer geobarometer. Nevertheless, the pressure range estimated for the lower crustal charnockitic xenoliths from the Spanish Central System (0.9–1.0 GPa; Villaseca *et al.*, 2007) may indicate the equilibrium conditions for these Cpx-III cores, as they are fragments from these xenoliths. Thus, the San Bartolomé de Pinares dyke carries xenocrystic Cpx-III and Cpx-II green core phenocrysts from lower crustal levels.

Pressure estimations, together with the strong overlap observed in Fig. 5 and 6 between the major element composition of rims from both clinopyroxene (the three studied types: Cpx-I-II-III) and amphibole with respect to that of corresponding groundmass phases from their host dykes, are in agreement with a process involving core formation within deep magma chambers, a quick melt evacuation and a last rim crystallization in subvolcanic conditions.

Nature of crystallising magmas

Different melts must have participated in the origin of clinopyroxene and amphibole phenocryst. To evaluate their cogenetism and their relationship with respect to the host alkaline dykes, we have calculated the composition of the melts in equilibrium with cores and rims using the partition coefficients of Hart & Dunn (1993) for clinopyroxene and LaTourrette *et al.* (1995) for amphibole, which have been determined on alkaline basalt and basanite liquids, respectively. The results have been represented in Fig. 9. The composition of melts in equilibrium with Cpx-I overlaps or is only slightly higher than that of SCS host dykes (Fig. 9A). Moreover, there are also similarities between the results obtained for amphibole cores and those of Cpx-I (Fig. 9B). These characteristics support that Cpx-I and amphibole phenocryst cores crystallised from liquids which are cogenetic with the parent magmas of the SCS alkaline dykes.

Clinopyroxene and amphibole from basic or ultrabasic rocks are usually incompatible trace element enriched phases which greatly control their behaviour during crystallization. Accordingly, co-precipitation of these minerals may strongly influence the distribution of trace elements between them. Although the existence of chemical equilibrium between coexisting Cpx-I cores and amphibole phenocrysts is difficult to evaluate, the similar trace element composition of melts in equilibrium with both minerals would indicate near equilibrium conditions. In Fig. 10 we have plotted averaged clinopyroxene-amphibole partition values for coexisting phases using cores with similar Mg#, bracketed within the short ranges of 0.70–0.75 for sample 103473 and 0.64–0.74 for sample 103818. These values might not be strictly interpreted as partition coefficients but can act as useful guides for trace element partitioning in alkaline magmatic rocks in general, and will be used here as an approximation.

The observed Cpx-I/amph trace element distribution is very similar in both samples (Fig. 10), with the only exception of slightly higher values for LREE, and lower for Rb in lamprophyre 103473 relative to 103818. These data indicate a clear control of amphibole for Rb, Ba, Ta, Nb and Sr partitioning over clinopyroxene, and they also suggest that Th, Zr, Hf, Y and REE would also preferentially enter amphibole structure, whilst clinopyroxene would only control U distribution (Fig. 10). Nevertheless, it should be noted that partitioning of Rb, Ba, Nb, Ta and Sr between clinopyroxene and amphibole in the considered samples is likely to be also influenced by phlogopite crystallization, as this mineral preferentially incorporate these elements rather than Th, U, Zr, Hf, Y or REE. In general, there are not big differences between our data and partition coefficients estimated for alkaline rock compositions and mantle enclaves. This resemblance with respect to literature values in similar magma compositions also supports the possibility outlined above that both Cpx-I and amphibole cores represent equilibrated crystallization products from the same alkaline magma.

The trace element compositional range of Cpx-II cores is very similar to that of Cpx-I, and the core to rim trace element variation displayed by both phenocrysts show a tendency of Cr-Ni depletion while LILE, HFSE and REE increase towards the rim (Table 4). This behaviour is in accordance with the fractionation of olivine + clinopyroxene + Cr-spinel ± Ti-rich phases deduced for major elements. The characteristic Mg-Cr enrichment of Cpx-II inner rims is accompanied by a weak depletion in the most incompatible trace elements, thus reinforcing the highly evolved nature of their cores and the mixing process involving hosting by a more primitive magma. Modelled melts in equilibrium with Cpx-II green cores are also similar in composition to those calculated for Cpx-I (Fig. 9C), thus indicating a possible genetic link. Tappe (2004) interpreted the presence of reversely zoned green-core clinopyroxenes within Mesozoic alkaline rocks from Scania as an evidence for the presence of evolved trace element enriched melts in the upper mantle. He established some genetic relationship between these crystals and previous Permo-Carboniferous lamprophyric dykes in the same region. But this reasoning is not possible in the Spanish Central System because of the inexistence of a previous alkaline magmatic event. It is also appreciable in Fig. 9 the similitude existing in the composition of the calculated parent melts of Cpx-I cores with respect to that of all rims (from Cpx-I, Cpx-II and

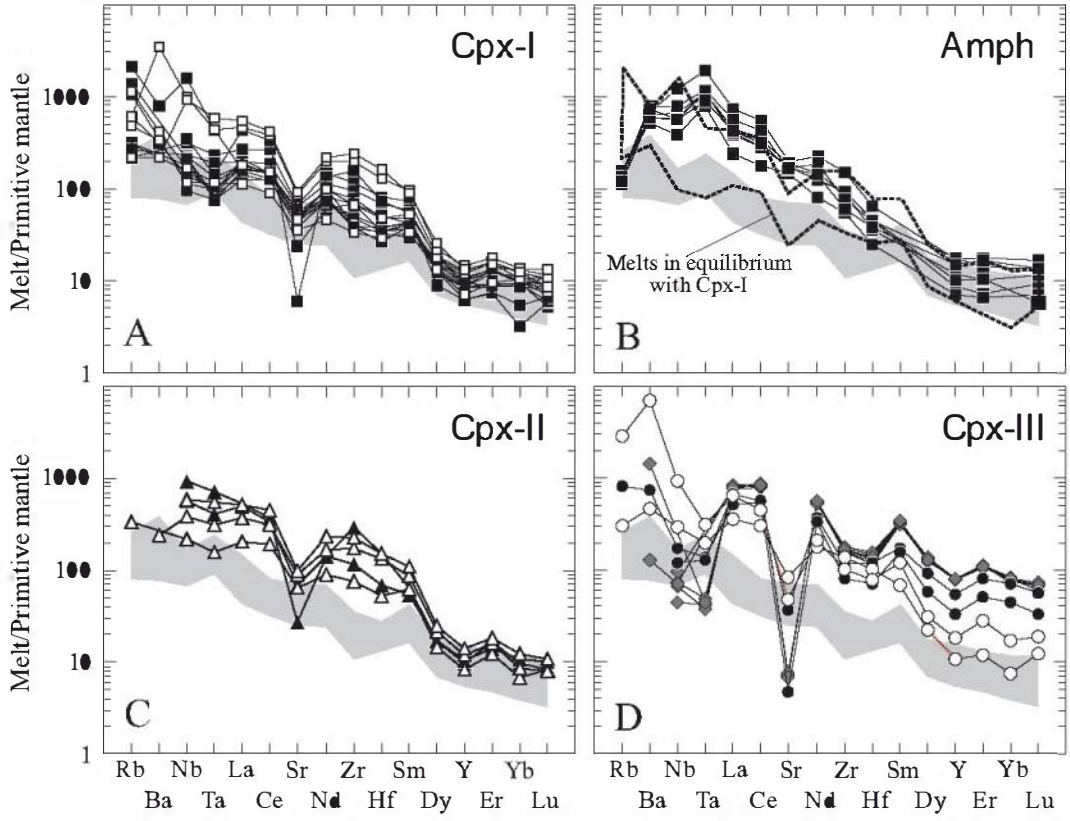

Fig. 9. Primitive mantle-normalised trace element composition of melts in equilibrium with clinopyroxene and amphibole phenocryst from Spanish Central System alkaline lamprophyres. Partition coefficients used are those of Hart & Dunn (1993) for clinopyroxene and LaTourrette *et al.* (1995) for amphibole. A: values for Cpx-I cores and rims. B: values for Amph phenocrysts. C: values for Cpx-II cores and rims. D: values for Cpx-III cores and rims, and also for cpx from charnockite xenoliths. The grey field represent the composition of SCS alkaline basic dykes (Villaseca *et al.*, 2004). See symbol legend in Fig. 7 for clinopyroxene and in Fig. 6 for amphibole. Normalising values after McDonough & Sun (1995).

Cpx-III). This reinforces that rims from all clinopyroxene phenocrysts would have formed from a single magma batch once all core types were incorporated into the host dykes.

On the contrary, melts in equilibrium with Cpx-III cores and clinopyroxenes from charnockite xenoliths show much higher contents in Y-REE and significant negative Eu, Sr and HFSE anomalies (Fig. 9D). These contents and their general normalised patterns are very different when compared to the SCS alkaline lamprophyres. They are probably genetically related with coexisting charnockite enclaves. The high modal proportion of plagioclase in these xenoliths and the absence of volatile-rich phases exclude the participation of lamprophyric magmas in their genesis and reinforce the xenocrystic origin of Cpx-III cores.

Calculated melts in equilibrium with Cpx-III display negative Zr-Hf anomalies and a strong Nb-Ta depletion with respect to LREE, which suggest parental magmas of calc-alkaline affinity. These parental magmas seem to have experienced a strong crystal fractionation process involving plagioclase, but also ilmenite, which is relatively abundant in the charnockite xenoliths and may be and important carrier of Nb and Ta (Green & Pearson, 1987). Apatite fractionation might be envisaged on the basis of the low fractionated chondrite-normalised REE pattern of Cpx-III. This

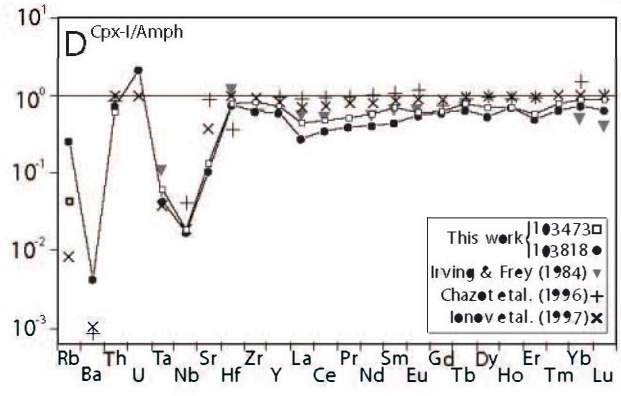

Fig. 10. Averaged clinopyroxene/amphibole trace element partition values for samples 103473 (Tornadizos outcrop) and 103818 (Muñotello outcrop). Data from empirical $D^{cpx/amph}$ trace element partition coefficients for alkaline basalts (Irving & Frey, 1984) and for mantle xenoliths (Chazot *et al.*,1996; Ionov *et al.*, 1997) are plotted for comparison.

is in accordance with Ionov *et al.* (1997) and Prowatke & Klemme (2006), which present apatite LREE-partition data much greater than for HREE.

Part of the charnockites from Villaseca *et al.* (2007) have been interpreted as lower crustal fragments formed as fractionates from calc-alkaline basic magmas. Thus, it is possible that the charnockite enclaves presented here (and also the accompanying Cpx-III xenocrysts) correspond with cumulates associated with highly evolved subalkaline magmas. In fact, the presence of mafic and ultramafic xenoliths from the lower crust, carried by the SCS alkaline dykes, has led some authors to think that a mafic underplating event might have developed to some degree at the base of the crust within the Spanish Central System, due to the accumulation of basic calc-alkaline melts at the end of the Hercynian orogeny (Orejana *et al.*, 2006).

Summary and conclusions

The SCS Permian alkaline lamprophyres show clinopyroxene and amphibole phenocrysts with complex normal and reverse zoning. Clinopyroxene phenocrysts with normal zoning (Cpx-I) are widespread distributed within the different dyke swarms, whereas clinopyroxenes with reverse zoning are restricted to the San Bartolomé de Pinares outcrop. In this latter dyke, Fe-rich green and colourless cores (Cpx-II and Cpx-III, respectively) represent crystallization from two distinct and more evolved liquids after significant fractional crystallization. Formation of rims with higher Mg# indicates mixing and incorporation into a third more primitive magma, giving rise to reverse zoning. This third melt is responsible for crystallization of clinopyroxene phenocrysts with normal zoning (Cpx-I). The fact that the rim compositions from all clinopyroxenes (with reverse and normal zoning) are similar and plot within a restricted range, indicates that they all crystallised from the same magma, close to its subvolcanic emplacement level. Amphibole phenocrysts from the Tornadizos and Hoyo de Pinares lamprophyres may have also been formed by magma mixing, though the melts involved must have shown less compositional contrast.

Taking into account the chemical composition of Cpx-I and Cpx-II cores, and also that of the melts in equilibrium with them, these crystals can be considered as derived from alkaline melts genetically related with the SCS alkaline magmatism. Estimated Cpx-I/Amph partition values are similar to literature partition coefficients from alkaline rocks, thus supporting that both phenocryst represent equilibrium conditions and were formed from similar magmas. On the contrary, Cpx-III cores show major and trace element contents in accordance with fractionation of plagioclase + clinopyroxene ± ilmenite ± apatite, and their composition resembles that of cpx from coexisting charnockite xenoliths, thus pointing to a xenocrystic origin. Cpx-III might derive from calc-alkaline deep cumulates, genetically related with other underplated metabasic rocks granulitized at lower crustal levels.

The coexistence of several clinopyroxene phenocryst types, together with granulite xenoliths, within the same thin section, points to the stagnation of the lamprophyric magmas at lower crustal depths and the eventual entrapment of the complex xenocryst and phenocryst mineral association during ascent.

Acknowledgements: We thank Alfredo Fernández Larios and José González del Tánago for their assistance with electron microprobe analyses. S. Conticelli, C. Wagner and S.F. Foley are thanked for their constructive review, which substantially improved the paper. LA-ICP-MS trace element mineral analyses were carried out at the University of Bristol and were funded by the *Access to Research Infrastructure action of the Improving Human Potential Programme* from the European Union; contract number PRI-CT-1999-00008. This study has been funded by the project CGL2004-02515 from the Spanish Ministry of Science and Education.

References

Aoki, K. & Kushiro, I. (1968): Some clinopyroxenes from ultramafic inclusions in Dreiser Weiher, Eifel. *Contrib. Mineral. Petrol.* **18**, 326-337.

Avanzinelli, R., Bindi, L., Menchetti, S., Conticelli, S. (2004): Crystallisation and genesis of peralkaline magmas from Pantelleria Volcano, Italy: an integrated petrological and crystal-chemical study. *Lithos* **73**, 41-69.

Bédard, J.H.J., Francis, D.M., Ludden, J. (1988): Petrology and pyroxene chemistry of Monteregian dykes: the origin of concentric zoning and green cores in clinopyroxenes from alkali basalts and lamprophyres. *Can. J. Earth Sci.* **25**, 2041-2058.

Brooks, C.K. & Printzlau, I. (1978): Magma mixing in mafic alkaline volcanic rocks: the evidence from relict phenocrysts phases and other inclusions. *J. Vol. Geotherm. Res.* **4**, 315-331.

Cellai, D., Conticelli, S., Menchetti, S. (1994): Crystal-chemistry of clinopyroxenes from potassic and ultrapotassic rocks in central Italy: implications on their genesis. *Contrib. Mineral. Petrol.* **116**, 301-315.

Chazot, G., Menzies, M.A., Harte, B. (1996): Determination of partition coefficients between apatite, clinopyroxene, amphibole, and melt in natural spinel lherzolites from Yemen: implications for wet melting of the lithospheric mantle. *Geochim et Cosmochim. Acta* **60**, 423-437.

Couch, S., Sparks, R.S.J., Carroll, M.R. (2001): Mineral disequilibrium in lavas explained by convective self-mixing in open magma chambers. *Nature* **411**, 1037-1039.

Dal Negro, A., Carbonin, S., Salviulo, G., Piccirillo, E.M., Cundari, A. (1985): Crystal chemestry and site configuration of the clinopyroxene from leucite-bearing rocks and related genetic significance: the Sabatini lavas, Roman Region, Italy. *J. Petrol.* **26**, 1027-1040.

Dal Negro, A., Cundari, A., Piccirillo, E.M., Molin, G.M., Uliana, D. (1986): Distintive crystal chemistry and site configuration of the clinopyroxene from alkali basaltic rocks: the Nyambeni clinopyroxene suite, Kenya. *Contrib. Mineral. Petrol.* **92**, 35-43.

Dobosi, G. & Fodor, R.V. (1992): Magma fractionation, replenishment, and mixing as inferred from green-core clinopyroxenes in Pliocene basanite, southern Slovakia. *Lithos* **28**, 133-150.

Duda, A. & Schmincke, H.-U. (1985): Polybaric differentiation of alkali basaltic magmas: evidence from green-core clinopyroxenes (Eifel, FRG). *Contrib. Mineral. Petrol.* **91**, 340-353.

Fernández Suárez, J., Arenas, R., Jeffries, T.E., Whitehouse, M.J., Villaseca, C. (2006): A U-Pb study of zircons from a lower crustal granulite xenolith of the Spanish Central system: a record of Iberian lithospheric evolution from the Neoproterozoic to the Triassic. *J. Geol.* **114**,471-483.

Francalanci, L., Davies, G., Lustenhouwer, W., Tommasini, S., Mason, P., Conticelli, S. (2005): Intra-grain Sr isotope evidence for crystal recycling and multiple magma reservoirs in the recent activity of Stromboli volcano, Southern Italy. *J. Petrol.* **46**, 1997-2021.

Green, T.H. & Pearson, N.J. (1987): An experimental study of Nb and Ta partitioning between Ti-rich minerals and silicate liquids at high pressure and temperature. *Geochim. Cosmochim. Acta* **51**, 55-62.

Hart, S.R. & Dunn, T. (1993): Experimental cpx/melt partitioning of 24 trace elements. *Contrib. Mineral. Petrol* **113**, 1-8.

Irving, A.J. & Frey, F.A. (1984): Trace element abundances in megacrysts and their host basalts; constraints on partition coefficients and megacryst genesis. *Geochim. Cosmochim. Acta* **48**, 1201-1221.

Ionov, D.A., Griffin, W.L., O'Reilly, S.Y. (1997): Volatile-bearing minerals and lithophile trace elements in the upper mantle. *Chem. Geol.* **141**, 153-184.

Kollárová, V. & Ivan, P. (2003): Zoned clinopyroxenes from Miocene basanite, Baská Stiavnica - Kalvária (Central Slovakia): indicators of complex magma evolution. *Slovak Geol. Mag.* **9**, 217-232.

Kushiro, I. (1969): Clinopyroxene solid solutions formed by reactions between diopside and plagioclase at high pressures. *Min. Soc. America, Special Paper* **2**, 179-191.

LaTourrette, T., Hervig, R.L., Holloway, J.R. (1995): Trace element partitioning between amphibole, phlogopite, and basanite melt. *Earth Planet. Sci. Lett.***135**, 13-30.

Markl, G. & White, C. (1999): Complex zoning between supercalcic pigeonite and augite from the Graveyard Point sill, Oregon: a record of the interplay between bulk and interstitial liquid fractionation. *Contrib. Mineral. Petrol.* **137**, 170-183.

McDonough, W.F. & Sun, S.S. (1995): The composition of the Earth. *Chem. Geol.* **120**, 223-253.

Neumann, E.-R., Wulff-Pedersen, E., Simonsen, S.L., Pearson, N.J., Martí, J., Mitjavila, J. (1999): Evidence for fractional crystallization of periodically refilled magma chambers in Tenerife, Canary Islands. *J. Petrol.* **40**, 1089-1123.

Nimis, P. & Ulmer, P. (1998): Clinopyroxene geobarometry of magmatic rocks Part 1: An expanded structural geobarometer for anhydrous and hydrous, basic and ultrabasic systems. *Contrib. Mineral. Petrol.* **133**, 122-135.

Orejana, D., Villaseca, C., Paterson, B.A. (2006): Geochemistry of pyroxenitic and hornblenditic xenoliths in alkaline lamprophyres from the Spanish Central System. *Lithos* **86**, 167-196.

Perini, G., Cebriá, J.M., López-Ruiz, J.M., Doblas, M. (2004): Carboniferous-Permian mafic magmatism in the Variscan belt of Spain and France: implications for mantle sources. in Permo-Carboniferous magmatism and rifting in Europe, Wilson, ed., M., Neumann E.R., Davies G.R., Timmerman M.J., Heeremans M., Larsen B., *Geol. Soc. London Spec. Publ.* **223**, London, 415-438.

Prowatke, S., Klemme, S. (2006): Trace element partitioning between apatite and silicate melts. *Geochim. Cosmochim. Acta* **70**, 4513-4527.

Shimizu, N. (1990): The oscillatory trace element zoning of augite phenocrysts. *Earth Sci. Rev.* **29**, 27-37.

Scarrow, J., Bea, F., Montero, P., Molina, J.F., Vaughan, A.P.M. (2006): A precise late Permian $^{40}Ar/^{39}Ar$ age for Central Iberian camptonitic lamprophyres. *Geol. Acta* **4**, 451-459.

Sun, S.S. & McDonough, W.F. (1989): Chemical and isotopic systematics of oceanic basalts; implications for mantle composition and processes. in Magmatism in ocean basins, ed. Saunders, A.D. & Norrey M.J., *Geol. Soc. Spec. Publ.* Blackwell Scientific Publications, Oxford, 313-345.

Tappe, S. (2004): Mesozoic mafic alkaline magmatism of southern Scandinavia. *Contrib. Mineral. Petrol.* **148**, 312-334.

Villaseca, C., Orejana, D., Pin, C., López García, J.A., Andonaegui, P. (2004): Le magmatisme basique hercynien et post-hercynien du Système Central Espagnol: essai de caractérisation des sources mantelliques. *C.R. Géosciences* **336**, 877-888.

Villaseca, C., Orejana, D., Paterson, B., Billström, K., Pérez-Soba, C. (2007): Metaluminous pyroxene-bearing granulite xenoliths from the lower continental crust in central Spain: their role in the genesis of Hercynian I-type granites. *Eur. J. Mineral.* **19**, 463-477.

Wagner, C., Mokhtari, A., Deloule, E., Chabaux, F. (2003): Carbonatite and alkaline magmatism in Taourirt (Morocco): petrological, geochemical and Sr-Nd isotope characteristics. *J. Petrol.* **44**, 937-965.

Wass, S.Y. (1979): Multiple origins of clinopyroxenes in alkali basaltic rocks. *Lithos* **12**, 115-132.

Xu, Y., Huang, X., Menzies, M.A., Wang, R. (2003): Highly magnesian olivines and green-core clinopyroxenes in ultrapotassic lavas from western Yunnan, China: evidence for a complex hybrid origin. *Eur. J. Mineral.* **15**, 965-975.

Yagi, K. & Onuma, K. (1967): The join $CaMgSi_2O_6$-$CaTiAl_2SiO_6$ and its bearing on the titanaugites. *J. Fac. Sci., Hokkaido Univ. (Series IV)* **13**, 117-138.